Anal. Bioanal. Electrochem., Vol. 13, No. 2, 2021, 214-225

Analytical & Bioanalytical Electrochemistry

Full Paper

Electro-oxidation of Formaldehyde on A Non-Platinum Metal/RGO Nanocomposite Modified Electrode in Alkaline Solution

Mohammad Ali Sheikh-Mohseni,[1,*] Vahdat Hassanzadeh,[2] and Biuck Habibi[2]

[1]Shahid Bakeri High Education Center of Miandoab, Urmia University, Urmia, I.R. Iran
[2]Electroanalytical Chemistry Laboratory, Department of Chemistry, Faculty of Sciences, Azarbaijan Shahid Madani University, Tabriz, Iran

*Corresponding Author, Tel.: +984445265960; Fax: +984445245725

E-Mail: m.sheikhmohseni@urmia.ac.ir

Received: 15 January 2021 / Received in revised form: 9 August 2021 / Accepted: 31 August 2021 / Published online: 30 September 2021

Abstract- Since the catalysis of formaldehyde oxidation is an important subject in fuel cells and also air and water purification, in this work a novel electrocatalyst was proposed for oxidation of formaldehyde. The electrocatalyst was constructed by electro-deposition of Ni and Co nanoparticles on the reduced graphene oxide (RGO) modified carbon paste electrode (NiCoRCPE). It was characterized by scanning electron microscopy, energy dispersive spectroscopy, X-ray diffraction and cyclic voltammetry. The electrocatalyst is worked by the mediation role of redox species of Ni nanoparticles in oxidation of formaldehyde. Also its ability enhanced by the synergetic effect of Ni and Co nanoparticles and the electrical properties of RGO. High current density and low over-potential for formaldehyde oxidation was obtained by the electrocatalyst. The current density is reached to 25 $mAcm^{-2}$ in 200 mM of formaldehyde. The onset potential of formaldehyde oxidation at the electrocatalyst become as 0.38V and its anodic peak as 0.75V versus SCE. Also, the catalytic reaction rate constant for the electro-oxidation of formaldehyde at the modified electrode was obtained as 55.6 $M^{-1} s^{-1}$. This high value for rate constant indicates the suitability of the proposed electrocatalyst for formaldehyde oxidation in fuel cells and purification applications.

Keywords- Nanostructures; Graphene; Electrocatalyst; Fuel cells; Purification

1. INTRODUCTION

The carbon nanostructured materials have various applications in different scientific fields [1-4]. Graphene, a famous member of that family, has concerned recently with the potential of a range of applications because of its excellent electronic, thermal, and mechanical properties [5,6]. Many methods have been developed for fabricating of graphene, such as mechanical cleavage [5,7]. But, one of the most capable methods, is reducing the graphene oxide (GO) in aqueous solution. GO, also generated by the oxidization and subsequent exfoliation of graphite. Practically, by fabricating reduced graphene oxide (RGO), electrically nonconductive GO transforms to highly conductive graphene [8]. The RGO has wide applications from chemistry and materials science to biology [9,10]. One of the most applications of RGO is its use in electrocatalysts structure [11-13].

Among different materials which can be used in electrocatalysts structure, nanomaterials and especially carbon and metal based nanomaterials have more advantages [14]. Often, the carbon nanomaterials have been used as supporting material and metal nanoparticles positioned on them as key parameter for catalytic process. Some metals such as Pt, Ru and Pt/Ru materials are generally used in electrocatalysts [15-17]. But, because of their high cost and also deactivation problem during working, researchers focused on using low cost metals such as Fe, Co, Ni, and Cu with appropriate electrocatalytic activity [18-21].

Nanostructured electrocatalysts can be used in different field such as sensing [22,23], energy conversion [24,25], purification [26] and also batteries [27]. Recently, more attention is paid to fuel cells because of their environmental and economic advantages [28]. For obtaining greatest results from fuel cells, an effective electrocatalyst should be used for electrocatalytic oxidation of fuel. On the other hand, a good electrocatalyst can be used in purification of air pollutants such as volatile organic compound (VOC) [29]. The VOCs can be oxidized to CO_2 by catalytic oxidation at an effective catalyst at lower temperatures than thermal oxidation [30].

The study of formaldehyde (HCHO) oxidation is important from different aspects. One of them is in fuel cell technology which the HCHO can be used as a fuel [31]. Another aspect is HCHO purification as an indoor air pollutant. Formaldehyde can emitted from building, furnishing, and consumer products. It cause to irritation of eyes and respiratory tract, headache, pneumonia, and even cancer [32]. Therefore, indoor HCHO purification is a great interest and the catalytic oxidation is one of the best methods for this purpose.

Many researches have been done for the oxidation of formaldehyde including platinum [33,34], copper [35,36], gold [37], palladium [38] and nickel [39,40] based electrodes. While, using of Ni and Co nanoparticles on the RGO substrate has not been reported yet. In this study, the reduced graphene oxide was fabricated at first. Then it was used for modifying carbon paste electrode to improve the electrical and charge transfer properties of the electrode. After that, the Ni and Co nanocomposite fabricate electrochemically on reduced graphene oxide carbon

paste electrode (NiCoRCPE). The structural and electrochemical characterizations of the obtained catalyst were studied. Because of importance of the formaldehyde oxidation, this oxidation was investigated at the prepared modified electrode as a non-platinum electrocatalyst.

2. EXPERIMENTAL SECTION

All electrochemical experiments were performed by a potentiostat/galvanostat (electro analyzer system, SAMA 500, I.R. Iran) in a three electrode cell system. A saturated calomel electrode (SCE), a platinum wire electrode and the reduced graphene oxide carbon paste (RCPE) based electrodes were used as reference, counter and working electrodes. Deionized water was used for preparation of all the solutions. The graphite fine powder and paraffin oil (DC 350, 0.88 gcm^{-3}) with high quality both from Merck (Germany). All other reagents were from Sigma-Aldrich with the maximum purity. The RGO was synthesized in our laboratory using an improved method [41].

The different carbon paste electrodes were prepared using a common method [14]. The RCPE was prepared by well mixing the RGO with graphite powder in the weight percent 5:100 and paraffin oil. Then, the RCPE was placed in a 10 mM solution of cobalt chloride and a potential of -0.95 V was applied for 450 s by chronoamperometry to obtain CoRCPE. This electrode was then inserted in a 10 mM nickel chloride solution and a potential of -1.25 V was applied for 200 s to obtain NiCoRCPE. The NiCoCPE was prepared in a same way but at bare CPE. Also, the NiRCPE was obtained in a same way but without deposition of Co.

3. RESULTS AND DISCUSSION

3.1. Structural characterization of NiCoRCPE

The structural, elemental and morphology characterizations of the prepared nanocomposite were investigated. The morphology of NiCoRCPE was studied by scanning electron microscopy (SEM) and energy dispersive X-ray spectroscopy mapping (EDX mapping), and its elemental analysis was performed by EDX. Also the X-ray diffraction (XRD) was used for confirming the structure of the synthesized nanocomposite.

Fig. 1A shows the XRD patterns of the RGO-CPE, NiRCPE and NiCoRCPE. The broad peak at 2θ value of about 20° in all XRD patterns corresponds to graphitic peak of RGO which indicates the presence of RGO on the electrodes. Also in three XRD patterns, the peaks at 27° and 55° corresponds to carbon (002) and (006), respectively, which related to the carbon paste as support material. The main peaks in the XRD pattern of the NiRCPE at 2θ values of 42.6º, 43.6º, 44.76º, 46.41º, 52º, 60.15º and 77.71º corresponding to (010), (002), (111), (011), (200), (012) and (220) crystal planes for Ni, respectively. In XRD patterns of the NiCoRCPE, the similar peaks have been seen which corresponding to pure Ni, pure Co or Ni-Co composite [42]. This similarity in XRD

pattern of NiRCPE and NiCoRCPE is conducted from sequential atomic number, close atomic weight and same crystal structure of the Ni and Co in the normal conditions.

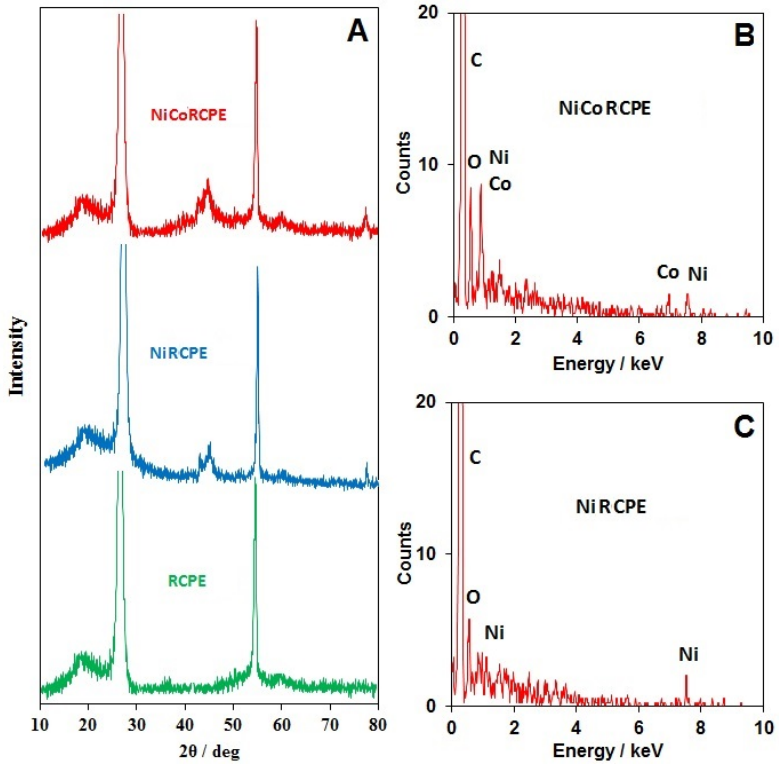

Fig. 1. A) XRD patterns of the RCPE, NiRCPE and NiCoRCPE; B) EDX spectrum of NiCoRCPE; C) EDX spectrum of NiRCPE

The elemental analysis of the NiCoRCPE and NiRCPE were performed by energy dispersive X-ray spectroscopy (EDX). Parts B and C of Fig. 1 show the EDX analysis results of the electrodes. The peaks of C, O and Ni were observed for both electrodes but the peaks of Co were seeing just in the EDX of NiCoRCPE (Fig. 1B and C).

Fig. 2A shows the SEM image of the NiCoRCPE surface. As can be seen, the Ni nanoparticles were grown on Co nanoparticles with regular distribution at NiCoRCPE. Also the nanoparticles are largely spherical in shape, indicates that the nanoparticles are not agglomerations. The nanoparticles show an approximately homogeneous dispersion with average particle size of 100 nm. The morphology of the electrodes surfaces was also investigated by EDX mapping (Fig. 2B). The results showed the formation of Ni and Co nanoparticles at NiCoRCPE with relatively regular distances between particles.

3.2. Electrochemically active surface area of the electrocatalyst

The electrochemically active surface area of the electrocatalyst and also the metal loading on it are important factors which affected the activity and yield of the electrocatalyst. Therefore, the real surface area of different electrodes was obtained using Randles-Sevcik equation in 1 mM of $K_4Fe(CN)_6/K_3Fe(CN)_6$ in 0.1M KCl solution, at first [43]. The approximately real

surface area was obtained as 0.208 cm^2 for NiCoRCPE, CoRCPE and NiRCPE, 0.191 cm^2 for NiCoCPE, CoCPE and NiCPE and 0.1 cm^2 for CPE. The real surface area of the electrodes with RGO and metal nanoparticles are increased more than two times.

The loading of the metal nanoparticles on the prepared electrocatalyst can be obtained by the columbic charge during the electro-deposition of nanoparticles [44]. The total metal nanoparticles loading on the NiCoRCPE was calculated as 27 µg and therefore the electrochemically active surface area of the NiCoRCPE is 0.77 m^2/g metal.

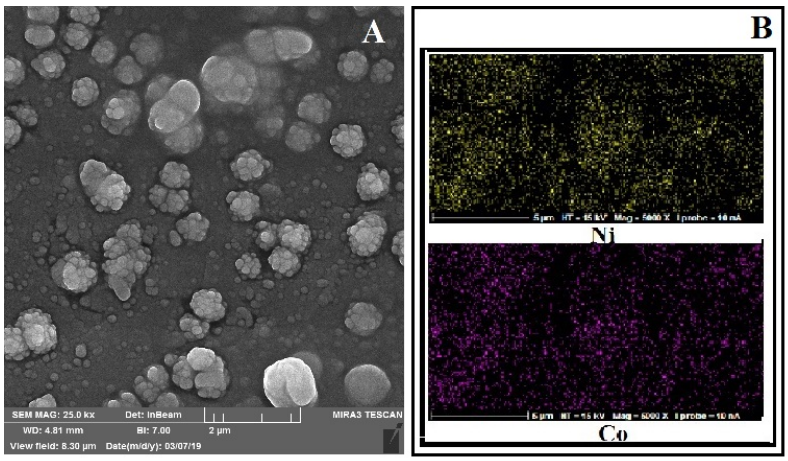

Fig. 2. A) SEM image of NiCoRCPE B) EDX mapping of NiCoRCPE

3.3. Electrochemical behavior of the electrocatalysts

The electrochemical behavior of the prepared electrocatalysts was investigated and compared by other electrodes by cyclic voltammetry. The obtained cyclic voltammograms in 0.1M NaOH solution at scan rate of 100 mVs^{-1} are presented in Fig.3. The NiRCPE shows a redox activity with anodic and cathodic peak at 0.45 V and 0.34 V, respectively (curve a), but, the CoRCPE has not any redox behavior in the same conditions (curve b). For NiRCPE when the potential is scanned anodically the Ni nanoparticles were oxidized to $Ni(OH)_2$ at lower potentials and then it can be oxidized to NiOOH at the potential of 0.45 V. Therefore, the observed redox behavior of NiRCPE is related to the oxidation and reduction of $Ni(OH)_2$/NiOOH redox couple [45,46].

The effect of the Co nanoparticles on the electrochemical behavior of the electrocatalyst can be seen from the cyclic voltammogram of NiCoRCPE (curve c in Fig. 3a). By the presence of Co nanoparticles in the structure of the electrocatalyst the electrochemical current of the redox activity of Ni is increased. Therefore, it can be concluded that more Ni nanoparticles are deposited on CoRCPE rather than RCPE. The comparison of curves c (NiCoRCPE) and d (NiCoCPE) shows the effect of RGO on the electrochemical response of the electrocatalyst. As can be seen, the RGO nanosheets increase the electrochemical current of the Ni

nanoparticles by the improving the conductivity and charge transfer properties of the CPE [9,12].

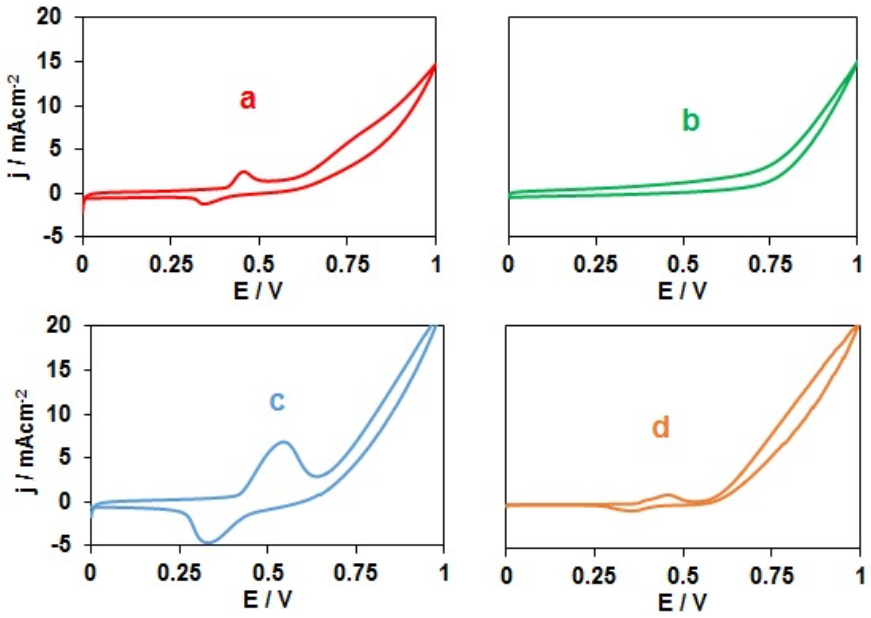

Fig. 3. Cyclic voltammograms of NiRCPE (curve a), CoRCPE (curve b), NiCoRCPE (curve c) and NiCoCPE (curve d) in 0.1M NaOH solution at scan rate of 100 mVs^{-1}

3.4. Oxidation of formaldehyde by electrocatalyst

As the oxidation of formaldehyde is the most important aim of the work, it was studied on the proposed electrocatalyst by CV. Fig. 4A shows the cyclic voltammograms of the NiCoRCPE in the absence and presence of formaldehyde and also the cyclic voltammogram of formaldehyde at bare CPE. The results show the formaldehyde cannot be oxidized at bare CPE to potential of 1 V (curve c). But the curve (a) shows formaldehyde begin to oxidation at the potential of 0.38V at NiCoRCPE and its anodic peak at this electrocatalyst is 0.75V. Curve b in Fig. 4A shows the cyclic voltammogram of NiCoRCPE in the absence of formaldehyde. As can be seen, the anodic peak current of $Ni(OH)_2$/NiOOH redox couple in NiCoRCPE is greatly enhanced in the presence of formaldehyde, because the formaldehyde reacts with the generated NiOOH on the electrode surface via a well-known mechanism as EC′ [47,48].

In Fig. 4B the catalytic activity of different modified electrodes are compared for formaldehyde oxidation. The cyclic voltammograms show that simultaneous presence of Ni and Co nanoparticles and RGO nanosheets in the electrode structure lead to the best catalytic activity where the oxidation current of formaldehyde greatly enhanced (Fig. 4B, curve a). Considering that the current density were used for plotting the cyclic voltammograms, therefore the difference observed between responses of formaldehyde oxidation on these electrodes is

not related to the difference of the electrodes surface area but is related to the synergistic catalytic role of Ni and Co nanoparticles and the good charge transfer properties of RGO.

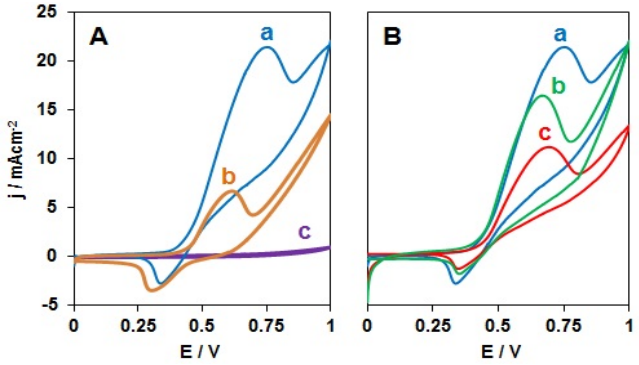

Fig. 4. A) Cyclic voltammograms of 0.05M formaldehyde at NiCoRCPE (curve a) and CPE (curve c), curve b is cyclic voltammogram of NiCoRCPE in the absence of formaldehyde; B) Cyclic voltammograms of 0.05M formaldehyde at NiCoRCPE (curve a), NiRCPE (curve b), NiCoCPE (curve c); Electrolyte: 0.1 M NaOH solution, scan rate: 100 mV s^{-1}

3.5. Investigation of potential scan rate and formaldehyde concentration on the catalytic process

The effect of the potential scan rate on the catalytic oxidation reaction of formaldehyde at NiCoRCPE was investigated. The obtained cyclic voltammograms of in 0.05M formaldehyde in different scan rates are shown in Fig. 5A. The inset of the figure displays the plot of formaldehyde anodic peak current density versus square root of potential scan rate. The linear behavior of this plot indicates that the electrocatalytic oxidation of formaldehyde is controlled by diffusion at NiCoRCPE. Also it can be seen by increasing the potential scan rate the cathodic peak current of $Ni(OH)_2$/NiOOH of the NiCoRCPE increased. This phenomenon has been happened because the reaction between formaldehyde and NiOOH cannot be occurred completely at high scan rate and therefore more NiOOH species stayed at the electrode surface to reduce to $Ni(OH)_2$. These observations confirmed the catalytic oxidation of formaldehyde via EC′ mechanism [47,48].

The effect of the concentrations of formaldehyde on the catalytic process was also investigated. The obtained cyclic voltammograms for different concentrations of formaldehyde are shown on Fig. 6. Part A in this figure indicates increasing the catalytic peak current density by the increasing of the formaldehyde concentrations from 10 mM to 50 mM. Part B of the figure shows that above the concentration of 50 mM the catalytic current is not increased very well. The behavior of the catalytic peak current toward the formaldehyde concentration is shown in Fig. 6C. This figure shows the best catalytic activity for formaldehyde oxidation is performed up to the concentration of 50 mM and it is suddenly dropped for upper concentrations. Because the active sites on the electrode surface is occupied by formaldehyde

molecules at high concentrations. Another observation is decreasing the cathodic peak current of the NiCoRCPE with increasing the formaldehyde concentration, so that the cathodic peak eliminate completely above the concentration of 100 mM. This phenomenon is related to the EC′ mechanism of the formaldehyde oxidation and it reason is that at high concentration of formaldehyde the more amounts of NiOOH is consumed at the electrode surface in the reaction with formaldehyde; therefore the reduction of NiOOH to $Ni(OH)_2$ cannot be performed.

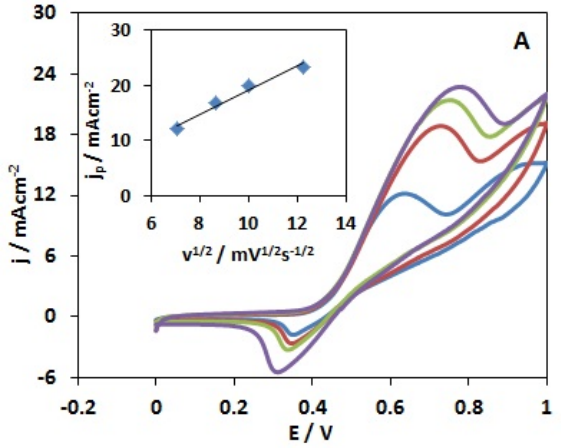

Fig. 5. Cyclic voltammograms of 0.05M formaldehyde at NiCoRCPE in different scan rates (from down to up: 50, 75, 100, 150 mVs^{-1}); inset shows the plot of anodic peak current density versus square root of potential scan rate

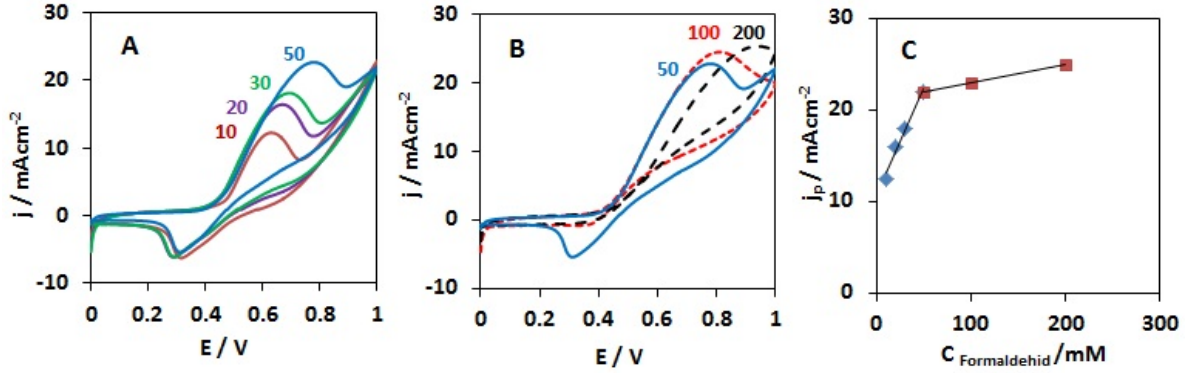

Fig. 6. Cyclic voltammograms of different concentration of formaldehyde at NiCoRCPE A) for 10, 20, 30 and 50 mM; B) for 50, 100 and 200 mM; C) plot of peak current density versus formaldehyde concentration

3.6. The catalytic reaction rate constant

The chronoamperometry technique was used for obtaining the catalytic reaction rate constant of formaldehyde at NiCoRCPE. Fig. 7 shows the chronoamperograms of various formaldehyde concentrations at NiCoRCPE with an applied potential step of 0.8 V.

The method of Galus was used for obtaining the catalytic rate constant [49]. In this method, simplicity, there is an equation between the ratio of catalytic and limited current (I_C/I_L) and the catalytic rate constant (k) as below equation**:**

$$I_C/I_L = \pi^{1/2}(kC_bt)^{1/2}$$

where, I_C is the catalytic current (the current of NiCoRCPE in the presence of formaldehyde), I_L is the limited current (the current of NiCoRCPE in the absence of formaldehyde), C_b is the bulk concentration of formaldehyde and t is the time. The inset of Fig.7 shows the plots of I_C/I_L versus $t^{1/2}$ for two concentrations of formaldehyde. From the slopes of these plots the average value of k was calculated as 55.6 $M^{-1}s^{-1}$ or 5.56×10^4 $cm^3mol^{-1}s^{-1}$. This high value indicates the great catalytic ability of the proposed electrocatalyst for formaldehyde oxidation.

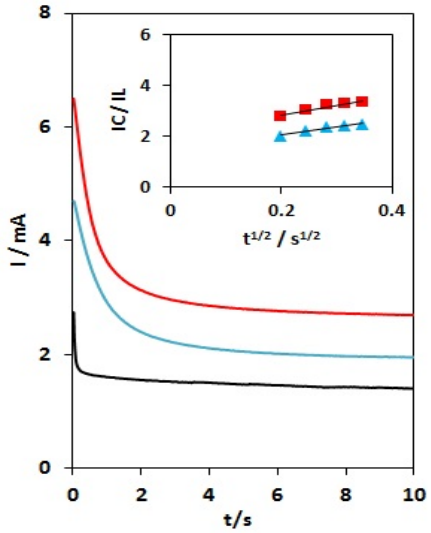

Fig. 7. Chronoamperograms of NiCoRCPE for different concentrations of formaldehyde (0.0, 0.05 and 0.1 M from down to up); Inset: plot of I_C/I_L versus $t^{1/2}$

Table 1. Comparison of some parameters of different modified electrodes for formaldehyde electro-oxidation

Electrode	Media	Ep (V)	Linear rang (mM)	Catalytic rate constant ($cm^3mol^{-1}s^{-1}$)	Ref.
Ni-TiO_2/CHIT/CPE [a]	0.1 M NaOH	0.5	0.28 – 25.0	-	[50]
Ni$(OH)_2$-X/CPE [b]	0.1 M NaOH	0.67	0.05 – 40	6.1×10^4	[51]
$NiWO_4$-NPs/CPE [c]	0.1 M NaOH	0.72	0.008 – 1	1.37×10^4	[52]
Ni/P-CPE [d]	0.1 M NaOH	0.6	0.02 – 11.5	-	[53]
NiPh/CF [e]	0.25 M KOH	0.5	-	2.59×10^7	[54]
Ni$(OH)_2$-MIL/CPE [f]	0.1 M NaOH	0.6	3 – 40	2.37×10^2	[55]
NiCoRCPE	0.1 M NaOH	0.62	10 – 200	5.56×10^4	This work

[a]Ni-TiO_2/chitosan modified carbon paste electrode; [b]Nickel(II) hydroxide-NaX nanozeolite modified carbon paste electrode; [c]Nickel tungstate nanoparticles modified carbon paste electrode; [d]Nickel doped P nanozeolite carbon paste electrode; [e]Nickel phosphate/carbon composite; [f]Ni$(OH)_2$-MIL-101(Cr) modified carbon paste electrode

The performance of NiCoRCPE is compared to other reported modified electrodes summarized in Table 1. The prepared electrode in this work shows some advantages for formaldehyde oxidation such as wide linear range, ability to catalyse the high concentration of formaldehyde, suitable over-potential and relatively high catalytic rate constant in comparison to several earlier reports. Additionally, the method for construction of NiCoRCPE related to other works is simple and low cost. Therefore, it can be concluded NiCoRCPE is an efficient electrocatalysts for the oxidation of formaldehyde.

4. CONCLUSION

In this work a novel electrocatalyst was proposed for oxidation of formaldehyde. The structure of the electrocatalyst, which contain Ni and Co nanoparticles and reduced graphene oxide (RGO, was characterized by scanning electron microscopy, energy dispersive spectroscopy, X-ray diffraction and cyclic voltammetry. The voltammetric results showed the mediated role of $Ni(OH)_2$/NiOOH redox couple in catalytic oxidation of formaldehyde. The synergetic effect of Co nanoparticles and RGO nanosheets in the electrocatalytic process enhanced the current density and decreased the overpotential for formaldehyde oxidation. Finally, this non-platinium electrocatalyst can be suggested for formaldehyde oxidation in fuel cells and purification applications.

Acknowledgements

The authors are grateful to the Urmia University and Azarbaijan Shahid Madani University for the financial support of the work.

REFERENCES

[1] P. Kumar, K. H. Kim, V. Bansal, and P. Kumar, Coord. Chem. Rev. 353 (2017) 113.

[2] M. Mazloum-Ardakani, M. A. Sheikh-Mohseni, and M. Salavati-Niasari, Electroanalysis 28 (2016) 1370.

[3] T. Rasheed, M. Adeel, F. Nabeel, M. Bilal, and H. M. Iqbal, Sci. Total Environ. 688 (2019) 299.

[4] M. S. Ghasemzadeh, and B. Akhlaghinia, Chemistry Select 31 (2019) 1542.

[5] A. G. Olabi, M. A. Abdelkareem, T. Wilberforce, and E. T. Sayed, Renew. Sustain. Energy Rev. 135 (2021) 110026.

[6] M. Li, T. Chen, J. J. Gooding, and J. Liu, ACS Sensors 4 (2019) 1732.

[7] Y. Wu, J. Zhu, and L. Huang, Carbon 143 (2019) 610.

[8] B. Ma, R. D. Rodriguez, A. Ruban, S. Pavlov, and E. Sheremet, Phys. Chem. Chem. Phys. 21 (2019) 10125.

[9] S. ul Haque, A. Nasar, and M. M. Rahman, Sci. Rep. 10 (2020) 1.

[10] A. Mondal, A. Prabhakaran, S. Gupta, and V. R. Subramanian, ACS Omega 6 (2021) 8734.
[11] M. K. Sahoo, and G. R. Rao, Chemistry Select 5 (2020) 3805.
[12] Y. R. Liu, X. Shang, W. K. Gao, B. Dong, J. Q. Chi, X. Li, K. L. Yan, Y. M. Chai, Y. Q. Liu, and C. G. Liu, Appl. Surf. Sci. 412 (2017) 138.
[13] J. Gu, X. Yin, X. Bo, and L. Guo, Chem. ElectroChem. 5 (2018) 2893.
[14] H. Imanzadeh, N. K. Bakirhan, B. Habibi, and S. A. Ozkan, J. Pharm. Biomed. Anal. 181 (2020) 113096.
[15] B. Habibi, H. Imanzadeh, Y. H. Shishavan, and M. Amiri, Catal. Lett. 150 (2020) 312.
[16] S. Yin, R. D. Kumar, H. Yu, C. Li, Z. Wang, Y. Xu, X. Li, L. Wang, and H. Wang, ACS Sustain. Chem. Eng. 7 (2019) 14867.
[17] S. Zhang, H. Rong, T. Yang, B. Bai, and J. Zhang, Chem. Eur. J. 26 (2019) 4025.
[18] S. R. Chowdhury, P. Mukherjee, and S. kumar Bhattachrya, Int. J. Hydrog. Energ. 41 (2016) 17072.
[19] K. Rahmani, and B. Habibi, Int. J. Hydrog. Energ. 45 (2020) 27263.
[20] L. Cao, Y. Shao, H. Pan, and Z. Lu, J. Phys. Chem. C. 124 (2020) 11301.
[21] H. Imanzadeh, and B. Habibi, Solid State Sci. 105 (2020) 106239.
[22] M. Mazloum-Ardakani, M. A. Sheikh-Mohseni, M. Abdollahi-Alibeik, and A. Benvidi, Sens. Actuators B 171 (2012) 380.
[23] M. A. Sheikh-Mohseni, and S. Pirsa, Electroanalysis 28 (2016) 2075.
[24] S. Ghosh, and R. N. Basu, Nanoscale 10 (2018) 11241.
[25] H. Mistry, A. S. Varela, S. Kühl, P. Strasser, and B. R. Cuenya, Nat. Rev. Mater. 1 (2016) 1.
[26] R. A. Hameed, and R. H. Tammam, Int. J. Hydrog. Energy 43 (2018) 20591.
[27] Y. Zhang, G. Xu, Q. Kang, L. Zhan, W. Tang, Y. Yu, K. Shen, H. Wang, X. Chu, J. Wang, and S. Zhao, J. Mater. Chem. 7 (2019) 16812.
[28] H. Yuan, and Q. Zhang, J. Energy Chem. 48 (2020) 107.
[29] M. Sun, Y. Zhang, H. H. Liu, F. Zhang, L. F. Zhai, and S. Wang, Environ. Int. 131 (20190) 104977.
[30] S. Dissanayake, N. Wasalathanthri, A. S. Amin, J. He, S. Poges, D. Rathnayake, and S. L. Suib, Appl. Catal. A 590 (2020) 117366.
[31] W. Liao, Y. W. Chen, Y. C. Liao, X. Y. Lin, S. Yau, J. J. Shyue, S. Y. Wu, and H. T. Chen, Electrochim. Acta 333 (2020) 135542.
[32] Y. Shen, F. Ning, Y. Zhan, C. Bai, and H. Wang, Appl. Catal. A 602 (2020) 117667.
[33] S. Zhao, Y. Wen, X. Peng, Y. Mi, X. Liu, Y. Liu, L. Zhuo, G. Hu, J. Luo, and X. Tang, J. Mater. Chem. A. 8 (2020) 8913.
[34] B. Habibi, and S. Ghaderi, Iran. J. Chem. Chem. Eng. 35 (2016) 99.
[35] S. Momeni, and F. Sedaghati, Microchem. J. 143 (2018) 64.
[36] S. Zhang, X. Wen, M. Long, J. Xi, J. Hu, and A. Tang, J. Alloys Compd. 829 (2020) 154568.
[37] D. Li, X. Zhang, J. Zhu, C. Wu, T. Zheng, C. Li, and M. Cao, Appl. Surf. Sci. 528 (2020) 146935.

[38] Pötzelberger, C. C. Mardare, W. Burgstaller, and A. W. Hassel, Appl. Catal. A Gen. 525 (2016) 110.
[39] S. K. Hassaninejad-Darzi, M. Rahimnejad, F. Shajie, and A. H. S. Kootenaei, Iran. J. Sci. Technol. Trans. A Sci. 42 (2018) 1259.
[40] Š. Trafela, J. Zavašnik, S. Šturm,and K. Ž. Rožman, Electrochim. Acta 362 (2020) 137180.
[41] D. C. Marcano, D. V. Kosynkin, J. M. Berlin, A. Sinitskii, Z. Sun, A. Slesarev, L. B. Alemany, W. Lu, and J. M. Tour, ACS Nano 4 (2010) 4806.
[42] B. Habibi, and N. Delnavaz, RSC Advances 6 (2016) 31797.
[43] B. Rezaei, and S. Damiri, Sens. Actuators B 134 (2008) 324.
[44] Y. D. Gamburg, and G. Zangari, Theory and practice of metal electrodeposition, Springer Science & Business Media (2011).
[45] L. R. Zhang, J. Zhao, M. Li, H. T. Ni, J. L. Zhang, X. M. Feng, Y. W. Ma, Q. L. Fan, X. Z. Wang, Z. Hu, and W. Huang, New. J. Chem. 36 (2012) 1108.
[46] R. M. A. Tehrani, and S. A. Ghani, Fuel Cells 9 (2009) 579.
[47] M. Mazloum-Ardakani, M. A. Sheikh-Mohseni, B. F. Mirjalili, and L. Zamani, J. Electroanal. Chem. 686 (2012) 12.
[48] A. J. Bard, and L. R. Faulkner, Electrochemical Methods Fundamentals and Applications, 2nd ed., Wiley, New York (2001).
[49] Z. Galus, Fundamentals of Electrochemical Analysis, Ellis Horwood, New York (1976).
[50] E. Zarei, M. R. Jamali, and J. Bagheri, Iran. J. Catal. 8 (2018) 165.
[51] S. Kavian, S. N. Azizi, and S. Ghasemi, Chin. J. Catal. 37 (2016) 159.
[52] S. Daemi, M. Moalem-Banhangi, S. Ghasemi, and A. A. Ashkarran, J. Electroanal. Chem. 848 (2019) 113270.
[53] S. N. Azizi, S. Ghasemi, and F. Amiripour, Sens. Actuators B 227 (2016) 1.
[54] S. A. Al-Jendan, W. Alarjan, I. Elghamry, A. Touny, M. M. Saleh, and M. E. Abdelsalam, Int. J. Hydrog. Energy 45 (2020) 14320.
[55] S. Gheytani, S. K. Hassaninejad-Darzi, and M. Taherimehr, Fuel Cells 20 (2020) 3.